Superstructures in arrays of rotated graphene layers: Electronic structure calculations

Eduardo Cisternas,[1] Marcos Flores,[2] and Patricio Vargas[1,*]
[1]*Departamento de Física, Universidad Técnica Federico Santa María, P.O. Box 110-V, 2340000 Valparaíso, Chile*
[2]*Atomic Physics Laboratory, RIKEN, Wako, Saitama 351-0198, Japan*
(Received 6 January 2008; revised manuscript received 22 July 2008; published 10 September 2008)

We have applied first-principles total-energy electronic structure calculations in the local-density approximation to obtain the spatial charge density for a three-layer graphene array with the top surface rotated by 21.8°. It is possible to identify superstructures over the rotated layer, known as moiré patterns, in this system. This kind of superstructure has been reported experimentally during scanning tunneling microscopy (STM) measurements. Within this framework, we show that the simulated STM images are strongly influenced by the relative rotation of the top layer with respect to the underlying graphite. In this particular case we relate the stacking sequence of atoms to the intensity maxima at different tip-surface distances.

DOI: 10.1103/PhysRevB.78.125406 PACS number(s): 71.15.Ap, 73.21.Cd, 68.37.Ef

I. INTRODUCTION

The acquisition of scanning tunneling microscopy (STM) images of highly oriented pyrolytic graphite (HOPG) surfaces with atomic resolution has been possible since the early 1980s. Additionally, many anomalous phenomena have been observed. One of these is superperiodicity, reported in the late 1980s by different groups.[1] In this case, the STM images show a periodicity from several to tens of nanometers over the original graphene layer. Some of the possible physical origins are multiple tip effects, foreign atom intercalation, immersion in aqueous solution,[2] moiré rotation pattern assumption,[3–6] etc. One hypothesis as to the origin of rotational moiré patterns is that they are a result of the rotated graphene layer on the bulk (underlying) graphene;[7] another relates the top surface with respect to the single graphite crystal. The second explanation is more widely accepted from many reports.

The first scheme was proposed by Kuwabara *et al.*[3] and was bolstered when Xhie *et al.*[5] showed the first experimental evidence in its favor and suggested that the result could be based on STM image formation theory for HOPG surfaces.[8] According to this theory, only the carbon atoms located in the β-type sites (atoms without neighbors in the adjacent layer) are visible for the STM because they present a local density of states (LDOS) greater than those located in the α-type sites (atoms with neighbors in the adjacent layer). Thus, a rotation in the top layer has the effect of generating regions that present different concentrations of β-type sites. Consequently, these regions will appear brilliant in STM images. Such regions were called g-β sites by Xhie *et al.*,[5] where g stands for "giant."

Rong and Kuiper[4] proposed an alternative explanation for the superstructures. From first-principles calculations of the density of states (DOS),[9] they showed that the current-density maxima are over regions that present a greater concentration of atoms with neighbors below them (g-α sites). Following this reasoning, a third region could be identified that presented a mixture of the two preceding ones, called "g-h sites," in reference to the "hollow" sites in graphite. Recently, Campanera *et al.*[6] used a geometrical algorithm to quantify the percentage of the different stacking sequences produced in a rotated two-layer graphene array and then, based on the DOS previously computed independently for these stacking sequences, not rotated, showed how the model of Rong and Kuiper works.

In this paper we study a three-layer graphene array with a rotated top layer. By applying a first-principles total-energy electronic structure calculation in the local-density approximation (LDA) to this rotated system, it is possible to identify superstructures in the obtained spatial charge density for this system. Within this framework, we show that the STM can detect the relative rotation of the top layer with respect to the underlying graphite and allow us to identify the stacking under the intensity maxima in this particular case.

II. CALCULATION METHOD

In this section we briefly describe the calculation method and the approximations used in this study. Using first-principles total-energy electronic structure calculations within the density-functional theory (DFT) (Ref. 10) and the LDA it is possible to obtain the spatial charge density above a graphite surface. In order to describe the electronic density of a surface retaining its inhomogeneities, we have performed detailed calculations of the graphene system. Our description is based on the *ab initio* linear muffin-tin orbital (LMTO) method, which is discussed elsewhere.[11] We define an energy window $[E_F - e|V|, E_F]$ to perform our calculations for the charge density and obtain a value that is, accepting the Tersoff-Hamann approximation,[12] proportional to the current density $j(\mathbf{r})$ detected by the STM tip.[13] Thus, defining the axis perpendicular to the graphene layers as the z axis and setting $z=0$ at the surface layer, we can compare our results with a STM image in the constant high mode for different values of z by mapping the calculated charge density in the corresponding x-y plane.

In order to compare our calculation with STM experimental data, we introduce radio tip effects by performing a lateral smoothing in the generated images. This smoothing consists of a window average of the tunneling current density around a neighbor region. We used a window of 1.2×1.2 Å^2. Our calculations are restricted to the filled states of the sample because in the DFT we find the lowest energy states, and as

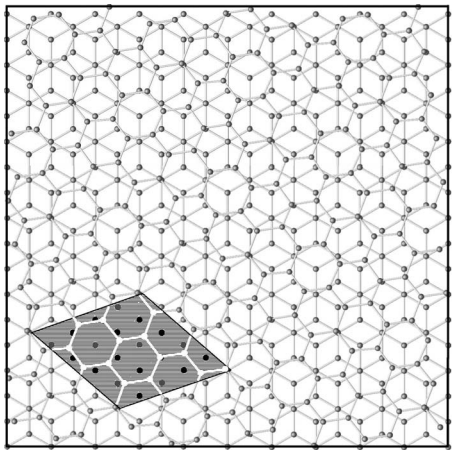

FIG. 1. Ball and stick model of an upper view of a 24×24 Å^2 region expanded for the three-layer unit supercell shown in the obscured region. The two lower layers present the usual *AB* stacking sequence of the bulk hexagonal graphite crystal (bottom layer in gray, middle layer in black); meanwhile the top layer presents a clockwise rotation angle of 21.8° (white).

a consequence of this, the calculated images can only be compared with experimental STM images in which the tip is biased positively with respect to the surface.

Geometry of the supercell

The three graphene layers exist in a slab model and the unit supercell is 20 Å high. This value represents a separation of about 14 Å between the top layer of a slab and the bottom layer of the slab above it, so that the slabs are substantially far apart to avoid electronic overlapping and we ensured that the charge density falls to zero in a wide region between them. Each slab is formed by 42 carbon atoms (14 atoms in each graphene layer), where two layers are arranged in the structure of the bulk hexagonal graphite crystal (with *AB* stacking); this means that the nearest in-layer carbon-carbon distance is 1.42 Å and the interlayer separation is 3.35 Å. The top layer presents a rotation angle of 21.8° around the α site. We restrict the study to this value because smaller angles give rise to larger superlattice constants and a greater number of atoms would be required for the unit supercell.

An upper view of the pattern expanded by this unit supercell is shown in Fig. 1. There is clearly an optical superstructure, which is known as a rotational moiré pattern. It is important to note that the rotational angle was measured clockwise, but due to the hexagonal symmetry of the lattice it is possible to identify a counterclockwise rotation angle that corresponds to 98.2°. The supercell unit appears in the obscured region, and only in this region is it possible to distinguish clearly atoms on different layers: bottom in gray, middle in black, and top in white.

The equations $D=d/[2\sin(\theta/2)]$ and $\phi=30°-\theta/2$ are known as the moiré equations, and they predict the behavior of the superstructure; here D is the superlattice periodicity, $d=2.46$ Å is the graphite lattice site constant, θ is the rotation angle, and ϕ is the inclination of the superlattice relative to the atomic lattice. It is easy to verify that the superstructure in Fig. 1 is consistent with $D=6.5$ Å and a counterclockwise inclination angle $\phi=19.1°$, in agreement with the moiré equations for a clockwise rotation angle of 21.8°.

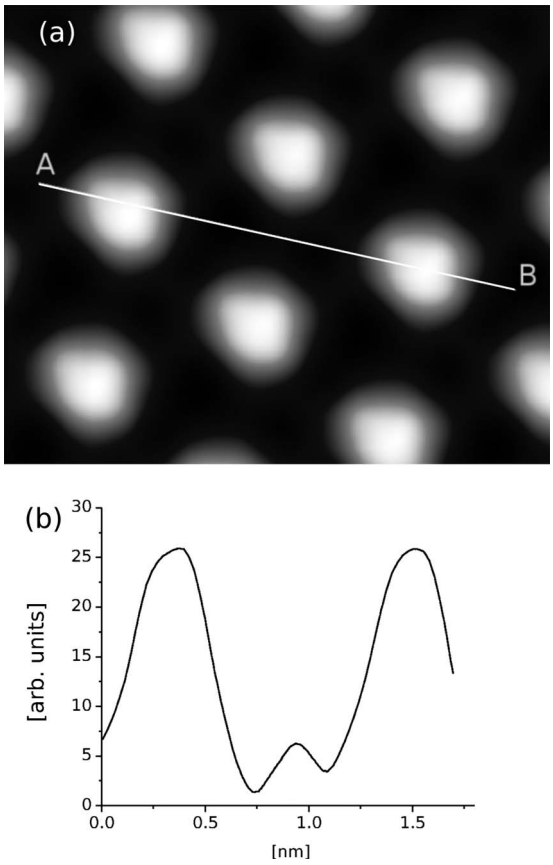

FIG. 2. (a) (19×16 Å^2) Image calculated for a bias voltage $V=1.0$ V in the constant high mode at a tip-surface separation of 3.0 Å. The superlattice constant is $D=6.5$ Å and its inclination angle is 19.1°. (b) Line profile along *A*-*B* in (a).

III. RESULTS

A. Charge density calculation

In Fig. 2(a) we show a 19×16 Å^2 charge-density image generated using the method described above with a bias voltage $V=1.0$ V and a constant tip-surface separation of 3.0 Å. The white (dark) regions represent high (low) charge density.

There are many clearly identifiable characteristics of the superstructure appearing in this image. First of all, it is easy to identify a triangular superstructure similar to those reported experimentally. This implies the existence of regions where higher electronic charge densities occur and they are ordered in a triangular pattern whose lattice constant is several times larger than the graphite lattice constant. For this particular case, the superlattice periodicity is $D=6.5$ Å, 2.65 times the lattice site constant for graphite, in agreement with the moiré formula. In addition, the superstructure presents a rotation angle of 19.1° with respect to an image of a normal graphite surface.

Finally, this image is directly associated with the superstructure indicated in Fig. 1. Similarly patterned images were verified for bias voltages $V=0.05$, 0.1, 0.2, and 0.5 V. However, at smaller bias voltages, the integral of spatial charge density diminishes and, consequently, smaller surface-tip separations are needed to detect the same tunneling current intensity.[13]

B. Line profiles

Figure 2(b) corresponds to a profile along the AB direction, shown in Fig. 2(a). The distance between the two current maxima is 11.3 Å, value that corresponds very well with the expected value of $D\sqrt{3}$, being $D=6.5$ Å, the superlattice constant. Figure 2(b) shows that the ratio between maximum and minimum values of charge densities is approximately 10. Thus, our calculations predict, under the Tersoff-Hamann model,[12] a STM image with sufficient contrast at a rotation angle of 21.8°. This angle is larger than 15° considered as the limit angle to obtain STM images with a moiré pattern with clear contrast by Campanera *et al.*[6] We return to this point in Sec. IV. However, it is interesting to note how our charge-density profile presents a similar behavior, at least in terms of shape, as experimental findings of the superstructures obtained on graphite in the constant current operation mode by Xhie *et al.*[5] and, in particular, by Rong and Kuiper.[4]

This last report[4] contains a profile very similar to Fig. 2(b), taken at 72 mV bias voltage; however, in the same experimental study, at 535 mV the secondary maximum disappears and the corrugation diminishes. Apparently, the tunneling current has been maintained as a constant, which means that the tip-surface separation is greater. In this way, if we calculate the charge density at 3.5 Å from the surface [Fig. 3(a)], we find that the superstructure retains the same characteristics as before, but this time with smaller charge maximum regions. On the other hand, a line profile was performed along the line indicated, and smaller charge-density variation was found [Fig. 3(b)], which would explain the smaller corrugation reported for 535 mV.[4] We have to stress that the maxima locations obtained for surface-tip separations of 3.0 and 3.5 Å coincide.

C. Maxima location

Figure 4 shows spatial charge-density plots integrated over a $[E_F, E_F-|e|V]$ window ($V=1.0$ V) for different planes, analogous to different tip-sample distances in STM current images. The planes are placed at (a) 1.0 Å, (b) 2.0 Å, (c) 2.5 Å, and (d) 3.0 Å, where the underlying atomic positions are revealed in order to identify over which regions the maxima are located. For easy identification, the atoms have been colored according to layer: blue for the atoms on the top rotated layer; green for the middle layer; and red for the bottom layer. Also the area enclosed by a black rectangle corresponds to (e), where the g-α and g-h sites were easily assigned according the notation of Xhie *et al.*[5] but where the g-β-site assignation is not possible because we could not ensure that there was a major concentration of atoms without the presence of neighbors below.

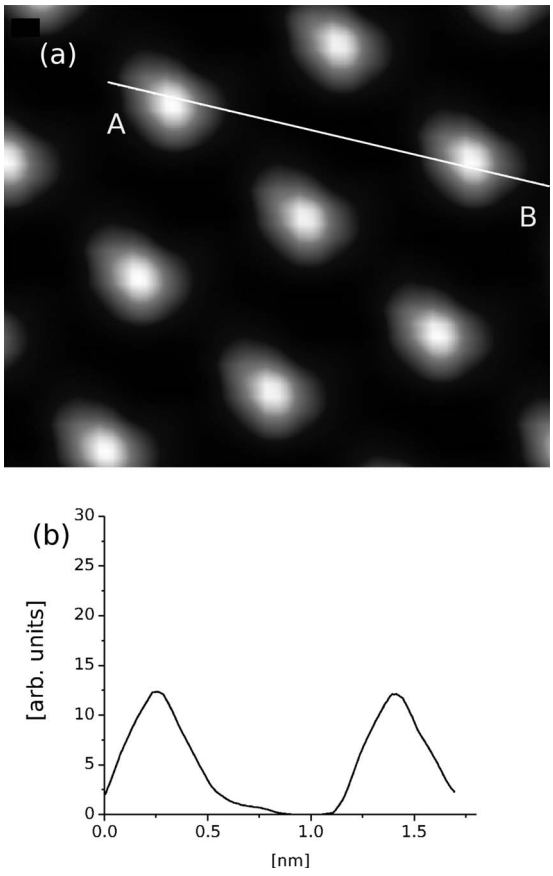

FIG. 3. (a) (19×16 Å^2) Image calculated for a bias voltage $V=1.0$ V in the constant high mode at a tip-surface separation of 3.5 Å. The superlattice constant is $D=6.5$ Å and its inclination angle is 19.1°. (b) Line profile along the line in (a).

Therefore we named it "g-delta site," as indicated in the Fig. 4(e).

Although it is possible to identify a superstructure with triangular symmetry in all images, for 1.0 Å the maximum is spread over an atom group on the upper-left border of the g-h site. It is interesting to note that this zone also presents a high concentration of atoms without neighbors below them.

For 2.0 Å it is possible to identify, in agreement with experiment,[14] two current maxima located in the upper border of the g-h site (primary maximum), which move for 2.5 Å to the right of the same g site in order to join with the secondary maximum forming a brilliant zone in the shape of a peanut. This peanut-shaped maximum transforms into a circular maximum, when the plane goes to 3.0 Å from the surface, located at the right of the g-h site. This location remains the same when the plane is located at 3.5 Å.

IV. DISCUSSION AND CONCLUSIONS

By means of first-principles total-energy electronic structure calculations and the Tersoff-Hamann theory,[12] we have generated charge-density images on planes located at different distances from a three-layer graphene array with a top layer rotated by 21.8°. This angle is larger than 15° considered as the limit angle to obtain STM images with a moiré

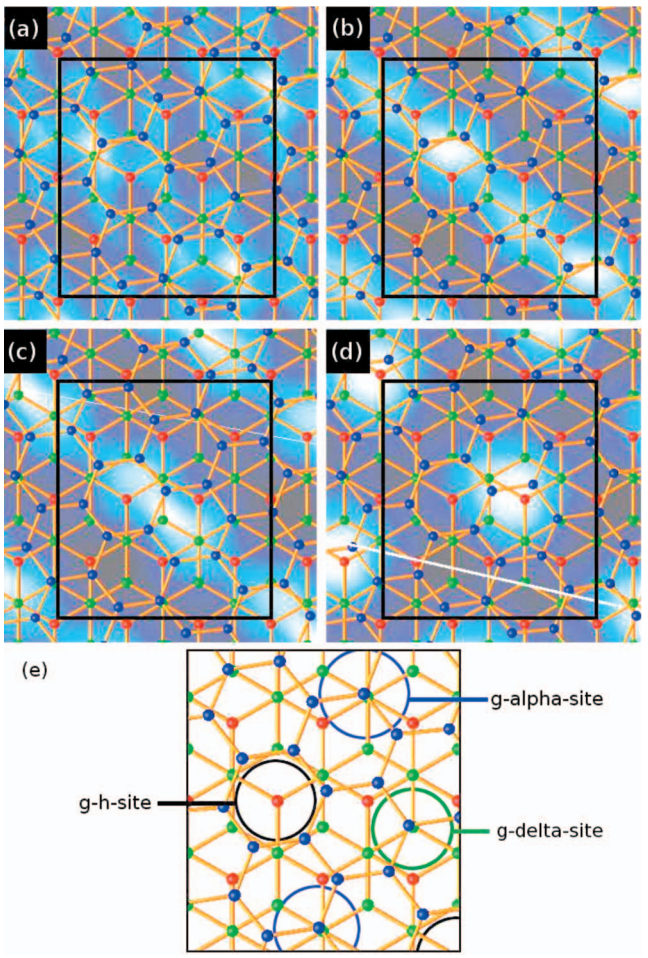

FIG. 4. (Color) Projection of charge density over the underlying atomic positions calculated for $V=1.0$ V and for (a) 1.0 Å, (b) 2.0 Å, (c) 2.5 Å, and (d) 3.0 Å over the surface layer. Atoms from the top layer are blue, those from the middle are green, and those in the bottom layer are red. The area enclosed by a black rectangle corresponds to (e), where the g site was assigned. Profiles were calculated along the segment indicated in the white line in (d) passing through the current maxima.

pattern with clear contrast by Campanera *et al.*[6] Therefore, to elucidate this issue we need an experimental verification, and our results should be compared with the constant height operation mode of STM images. There is some indirect experimental evidence about moiré pattern formation for angles larger than 15°.[15]

The calculated images show superstructures for planes located at distances larger than 3.0 Å and are in very good agreement with experimental results reported previously for STM on graphite.[4,5,16–18] In particular, accepting that the local current density at constant height STM operation mode and the tip-surface distance at constant current STM operation mode are directly proportional to each other, we can compare line profiles of our calculated images with corrugation reported experimentally. This agreement indicates that the phenomenon has a purely electronic origin and that the deformations in the top layer due to mechanical interaction with the STM tip are not relevant.[4,5,16,18] Moreover, these results show that the STM can detect misorientation between the top and the internal layers in graphite, where the interactions between layers are very weak. For the same reason, the simulation of a more realistic system would require enough numbers of graphene layers on the slab (in order to ensure that all these weak interactions among layers are considered and the graphite surface is correctly represented) and a top misoriented graphene layer as it was introduced here.

In our simulated results, the positions of the atoms under the calculated STM images are known and therefore it is possible to verify directly the stacking sequence under the current intensity maxima. Nevertheless, from the common assignation for g sites,[5] it is clear that the charge-density maxima are not located on these sites. This could be due to the fact that this assignation will be different if we choose a larger region enclosed in the circles in Fig. 4(e). This is the case of the g-h and g-α sites, for example, where a larger circle incorporates several atoms without a neighbor below. This made the assignation of the g-β site even more difficult. To elucidate this point it would be necessary to perform calculations for lower angles.

The shifting of position maxima on charge density as a function of distance from the surface is evidence of the spatial dependence of the surface wave functions of electrons, which contribute to the charge density [Eq. (2.2b) of Ref. 19]. Further, the maxima provide evidence of quantum interference effects, but the details of the maxima location require a more accurate analysis. Moreover, the STM results show an increasing resolution for smaller tip-surface distance in agreement with the Tersoff-Hamann model.[12]

The majority of the electronic states that form the charge density are surface states. Our system is built up using three graphene layers; therefore, it is mainly a surface system, not a bulk system.

Finally, this study opens the possibility of an extension of these calculations, for instance, through the introduction of defects, as vacancies or edges, in the rotated surface layer of the system. Rong[20] has experimentally shown that the presence of vacancies in the surface layer induces the disappearance of its corresponding moiré maximum in what is known as a supervacancy. Also, the abrupt completion of the superficial layer produces an edge, which has a strong influence on the superstructure depending on its shape: zigzag, armchair, or a mixture of both.[21]

In conclusion, the moiré pattern of the three-layer graphene array, where the topmost is misoriented, was reproduced by applied first-principles total-energy electronic structure calculations. In addition, some experimental features from STM observations were reproduced.

ACKNOWLEDGMENTS

This work was partially supported by MECESUP under Grant No. USA-0108, Fondecyt under Grant No. 1070224, and Millennium Science Initiative under Project No. P06-022-F.

*patricio.vargas@usm.cl

[1] J. W. Lyding, J. S. Hubacek, G. Gammie, S. Skalaand, and R. Brockenbrough, J. Vac. Sci. Technol. A **6**, 363 (1988); T. Hashizume, I. Kamiya, Y. Hasegawa, N. Sano, T. Sakurai, and H. W. Pickering, J. Microsc. **152**, 347 (1988); V. Elings and F. Wudl, J. Vac. Sci. Technol. A **6**, 412 (1988).

[2] V. J. Cee, D. L. Patrick, and T. P. Beebe, Jr., Surf. Sci. **329**, 141 (1995); Y. Wang, Y. Ye, and K. Wu, *ibid.* **600**, 729 (2006).

[3] M. Kuwabara, D. R. Clarke, and D. A. Smith, Appl. Phys. Lett. **56**, 2396 (1990).

[4] Z. Y. Rong and P. Kuiper, Phys. Rev. B **48**, 17427 (1993).

[5] J. Xhie, K. Sattler, M. Ge, and N. Venkateswaran, Phys. Rev. B **47**, 15835 (1993).

[6] J. M. Campanera, G. Savini, I. Suarez-Martinez, and M. I. Heggie, Phys. Rev. B **75**, 235449 (2007).

[7] K. Kobayashi, Phys. Rev. B **53**, 11091 (1996).

[8] D. Tománek, S. G. Louie, H. J. Mamin, D. W. Abraham, R. E. Thomson, E. Ganz, and J. Clarke, Phys. Rev. B **35**, 7790 (1987).

[9] J.-C. Charlier, J.-P. Michenaud, and X. Gonze, Phys. Rev. B **46**, 4531 (1992).

[10] P. Hohenberg and W. Kohn, Phys. Rev. **136**, B864 (1964); W. Kohn and L. J. Sham, *ibid.* **140**, A1133 (1965).

[11] O. K. Andersen and O. Jepsen, Phys. Rev. Lett. **53**, 2571 (1984); O. K. Andersen, O. Jepsen, and D. Gloetzel, in *Highlights of Condensed Matter Theory*, edited by F. Bassani, F. Fumi, and M. P. Tosi (North-Holland, New York, 1985); O. K. Andersen, O. Jepsen, and M. Sob, in *Electronic Band Structure and its Applications*, Lecture Notes in Physics, edited by M. Yussouff (Springer-Verlag, Berlin, 1987); O. K. Andersen, Z. Pawlowska, and O. Jepsen, Phys. Rev. B **34**, 5253 (1986).

[12] J. Tersoff and D. R. Hamann, Phys. Rev. Lett. **50**, 1998 (1983).

[13] A. Selloni, P. Carnevali, E. Tosatti, and C. D. Chen, Phys. Rev. B **31**, 2602 (1985).

[14] T. M. Bernhardt, B. Kaiser, and K. Rademann, Surf. Sci. **408**, 86 (1998).

[15] Y. Gan, W. Chu, and L. Qiao, Surf. Sci. **539**, 120 (2003).

[16] W.-T. Pong, J. Bendall, and C. Durkan, Surf. Sci. **601**, 498 (2007).

[17] W.-T. Pong, J. Bendall, and C. Durkan, Jpn. J. Appl. Phys., Part 1 **44**, 5443 (2005).

[18] W.-T. Pong and C. Durkam, J. Phys. D **38**, R329 (2005).

[19] D. Tomanek and S. G. Louie, Phys. Rev. B **37**, 8327 (1988).

[20] Z. Y. Rong, Phys. Rev. B **50**, 1839 (1994).

[21] Y. Niimi, T. Matsui, H. Kambara, K. Tagami, M. Tsukada, and H. Fukuyama, Phys. Rev. B **73**, 085421 (2006); Y. Kobayashi, K. I. Fukui, T. Enoki, and K. Kusakabe, *ibid.* **73**, 125415 (2006).